M2Or3J-02

Cryogenic vacuum chamber testing of a conductively-cooled, high temperature superconducting rotor for a 1.4 MW electric machine for aeronautics applications

Justin J. Scheidler[1], Erik J. Stalcup[1], Thomas F. Tallerico[1], William Torres[2], Kirsten P. Duffy[3], Tysen T. Mulder[1]

[1] NASA Glenn Research Center

[2] Wolf Creek Federal Services

[3] University of Toledo

Motivation

- Aviation impacts:

Climate
- **CO_2** (dominant), **contrails** (~$\frac{1}{2}$ impact of CO_2), **H_2O vapor, soot**

Environment
- Air quality – **NO_x** (dominant), **sulfur**
- Noise

- Despite significant progress in efficiency, global CO_2 emissions from aviation growing at increasing rate
- 2 options:
  - Change fuel (e.g., jet A → SAF or H_2)
  - Electrify
- NASA's High-Efficiency Megawatt Motor (HEMM) sized as generator for NASA's STARC-ABL concept

Global aviation impact on CO_2 (data from [1])

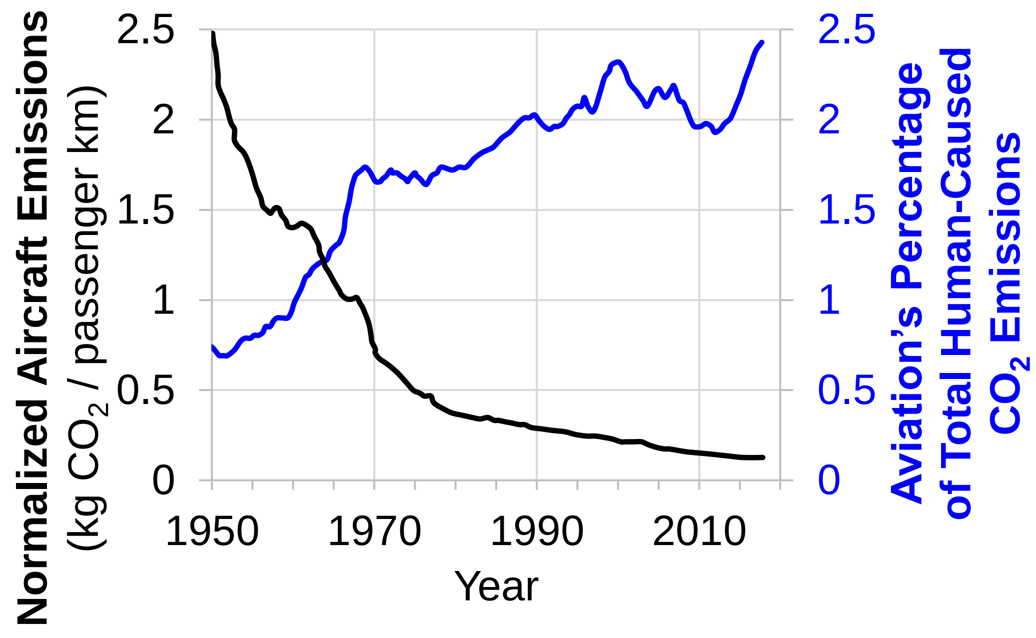

STARC-ABL

1. Lee, D.S. et al., Atmospheric Environment 244, 117834, 2021.

NASA's High-Efficiency Megawatt Motor (HEMM)

Parameter	Value
Rated continuous power	1.42 MW
Nominal speed	6,800 rpm
Tip speed	107 m/s
Rated torque	2 kNm
Electromagnetic specific power goal	16 kW/kg
Efficiency goal	> 98%

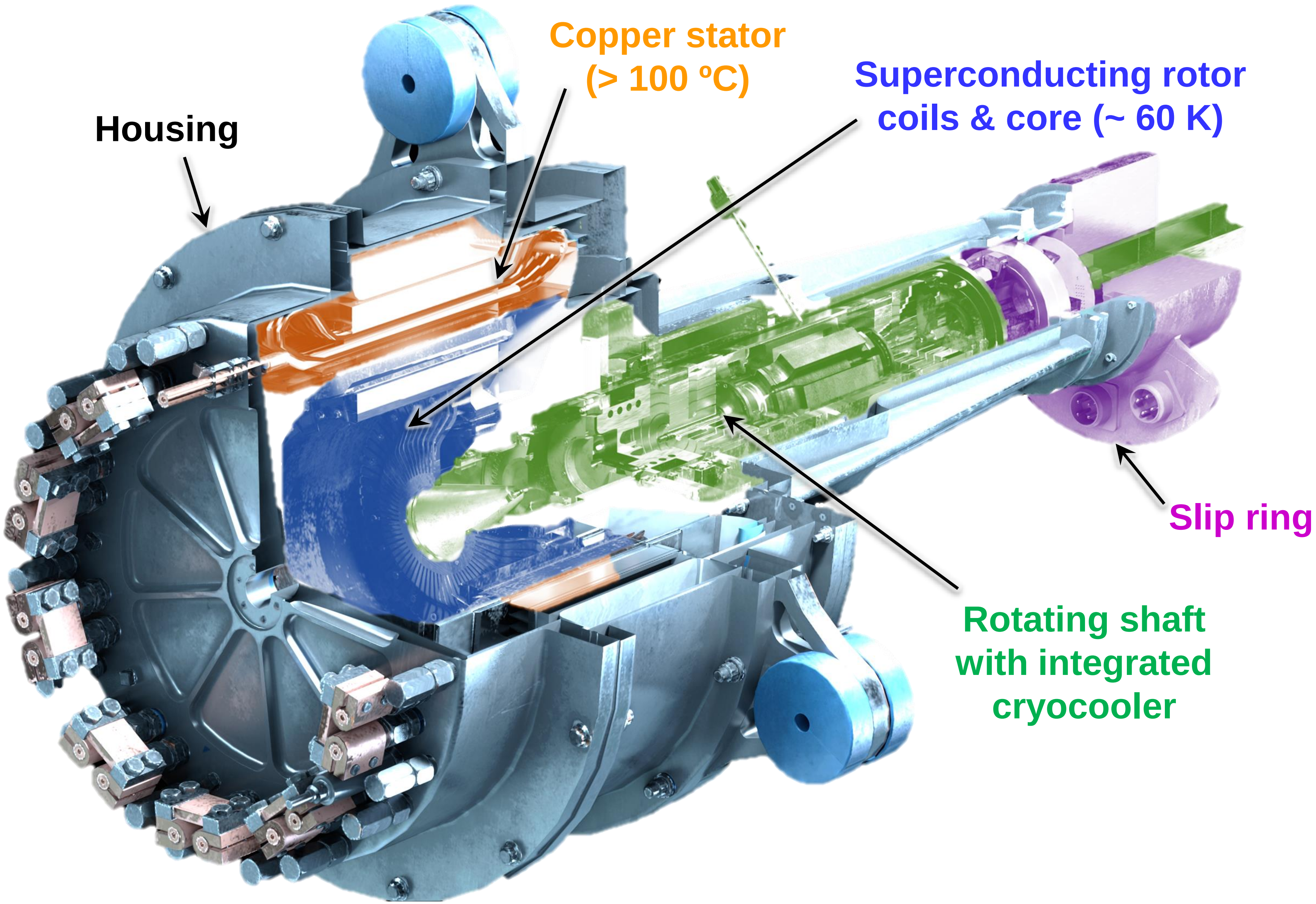

HEMM's Superconducting Rotor

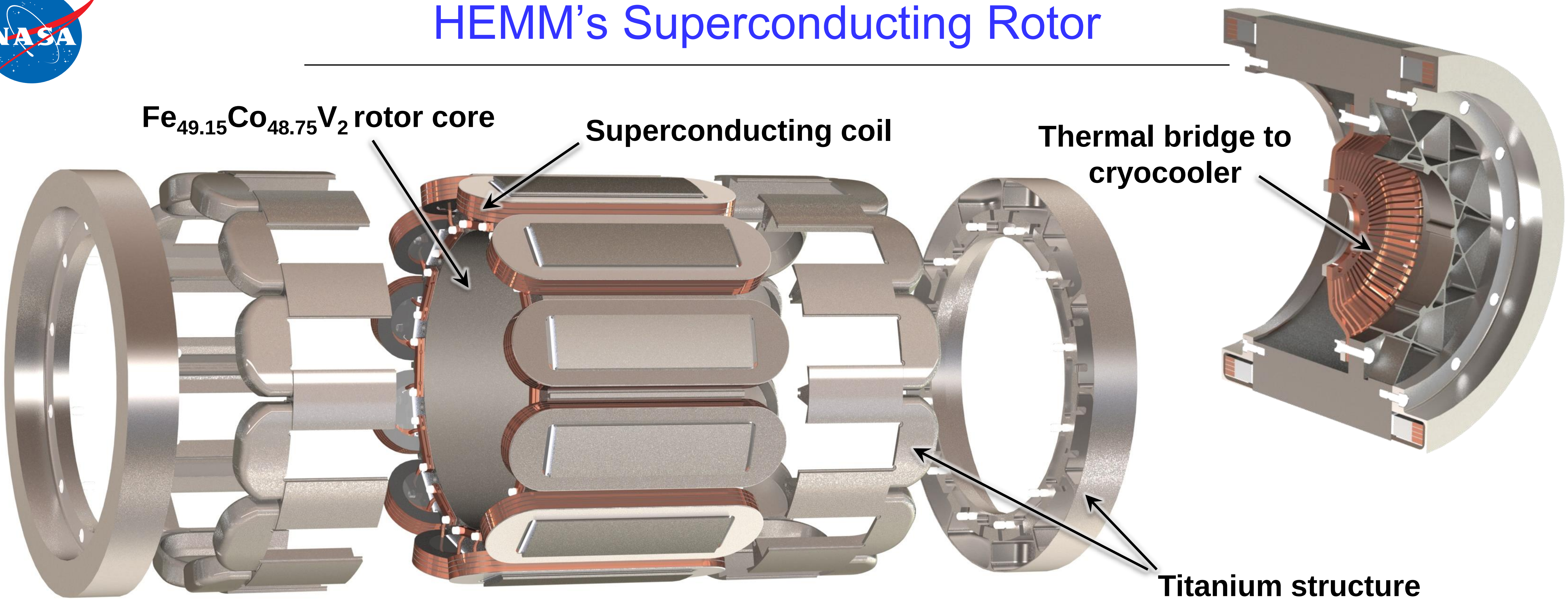

Parameter	Value
Pressure of rotor cavity	< 1e-3 torr
# poles (coils)	12
Superconductor	2^{nd} generation high temperature superconductor

Parameter	Value
Coil configuration	No-insulation quadruple pancake
# turns per coil	600 (150 per layer)

Experimental Setup – Physical Assembly

- Used NASA Glenn's ICE-Box

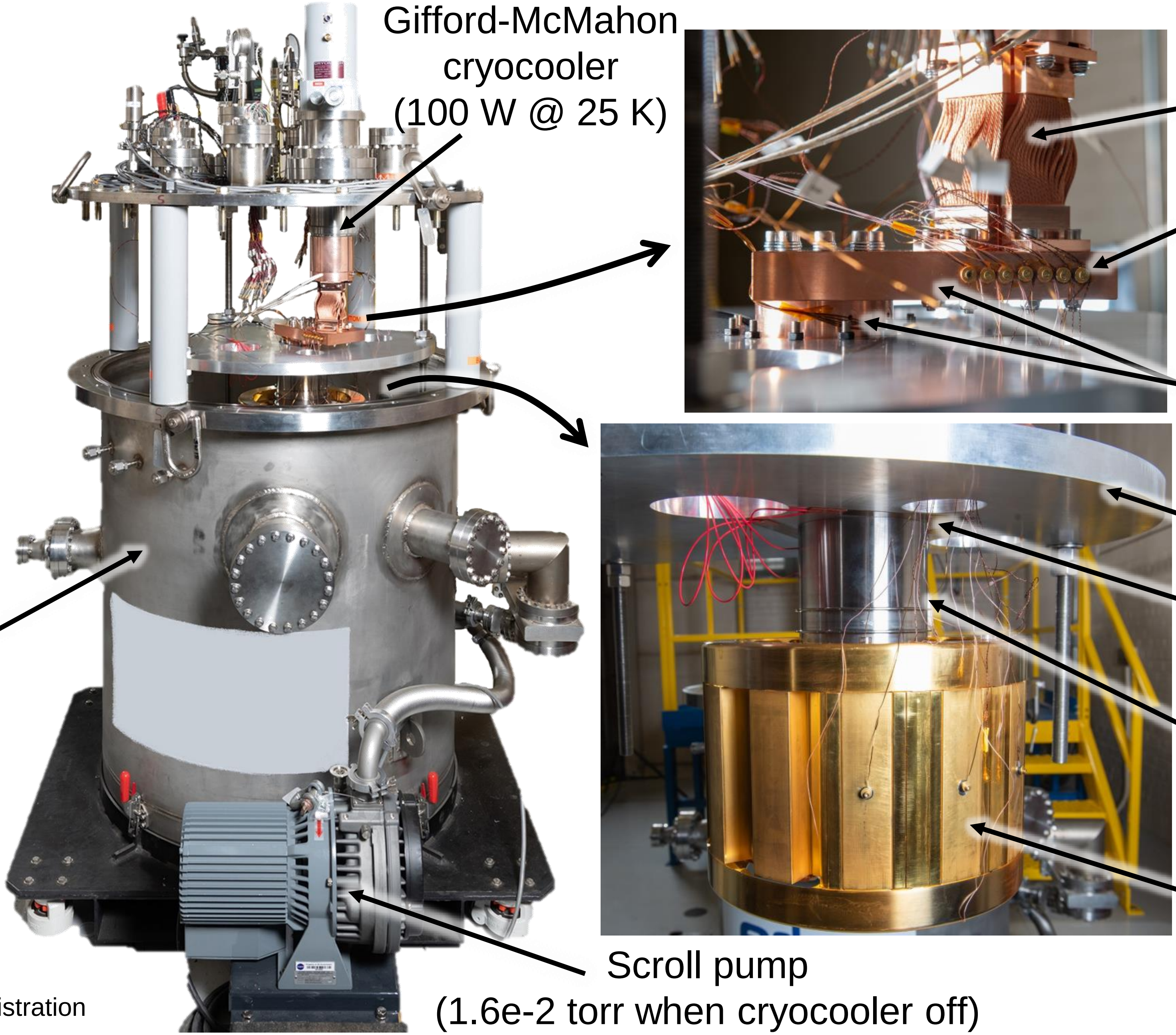

Experimental Setup – Physical Assembly

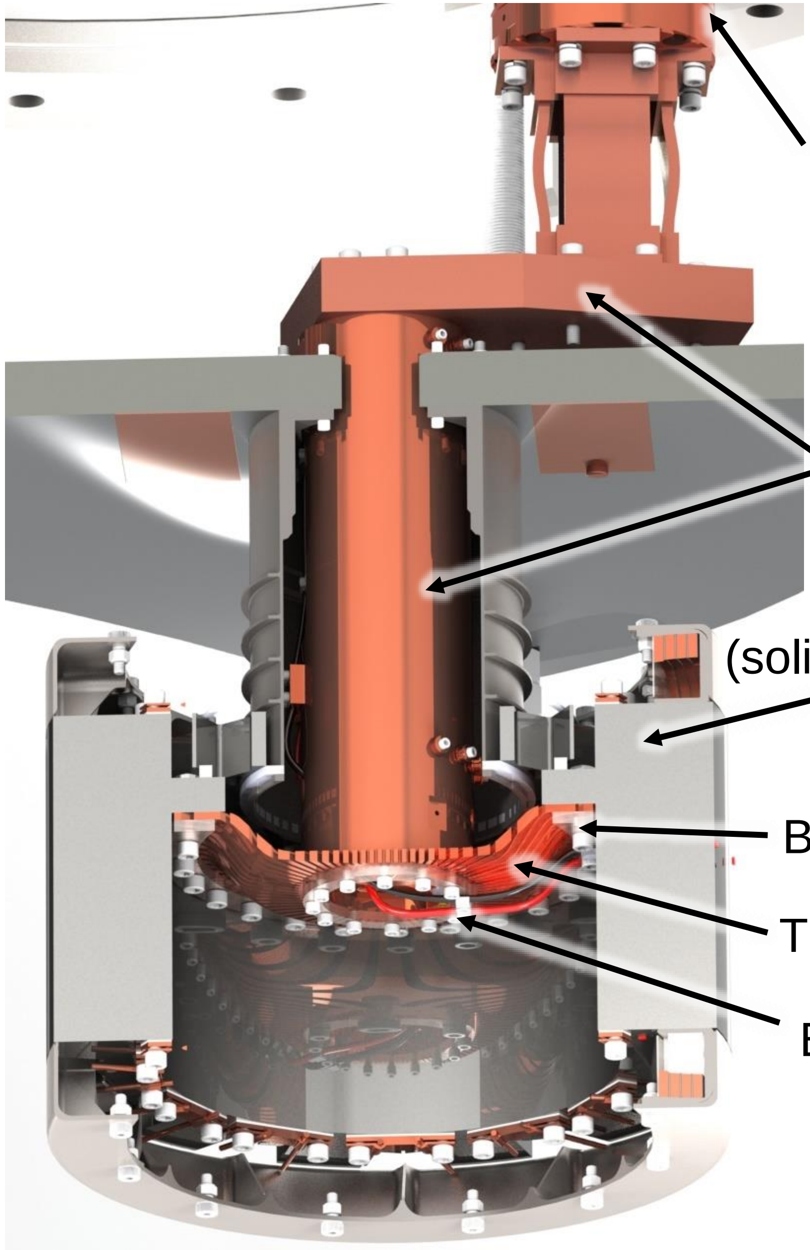

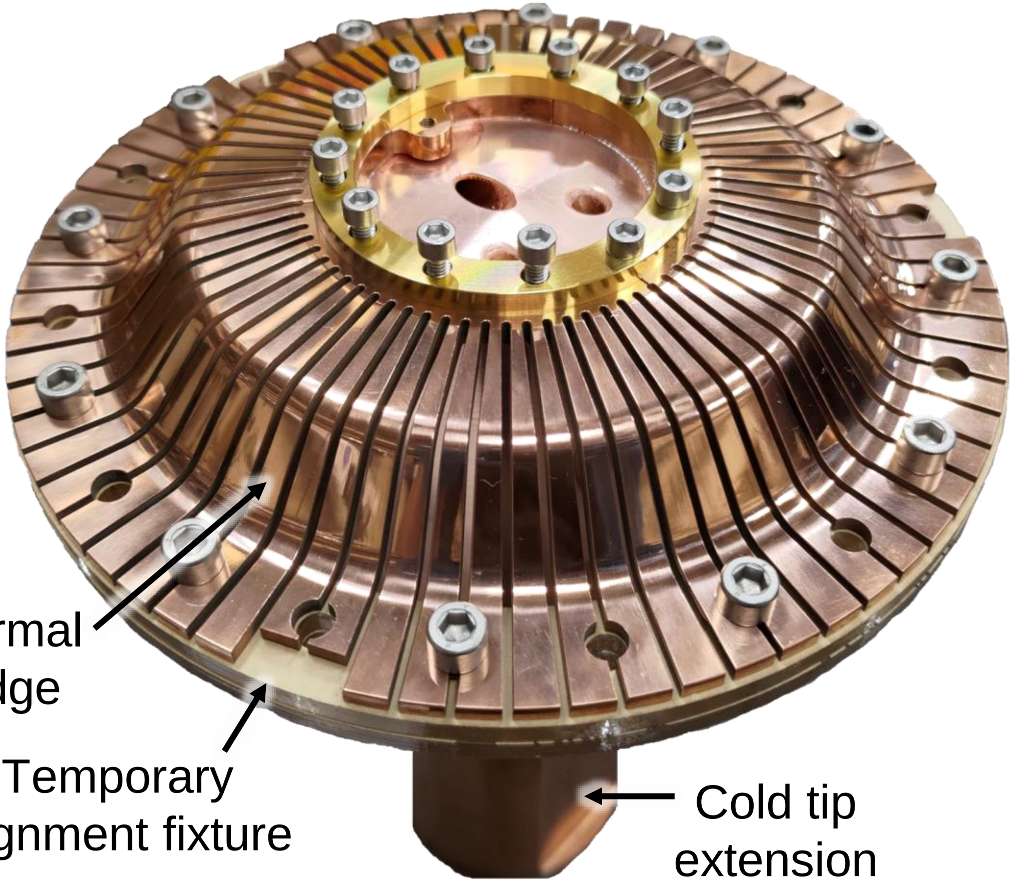

Experimental Setup – Physical Assembly

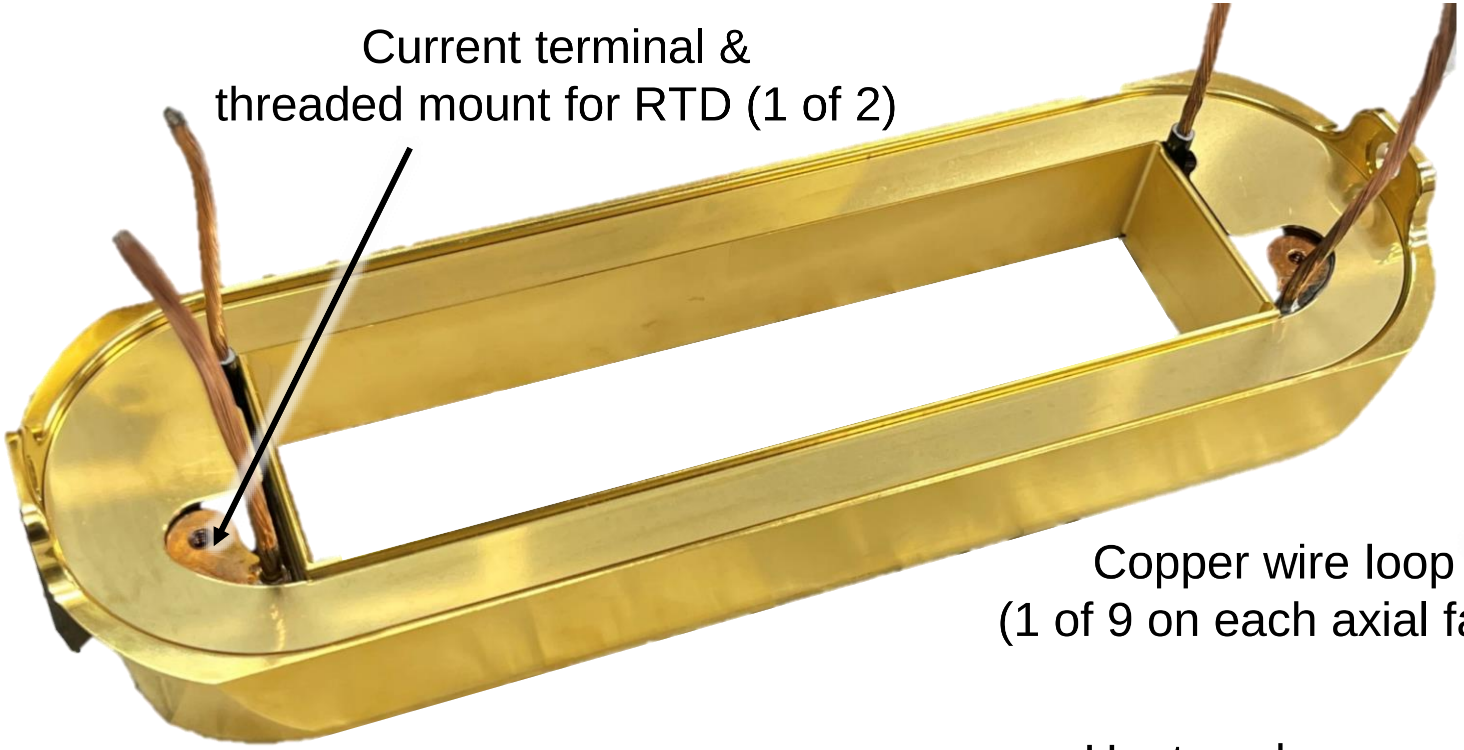

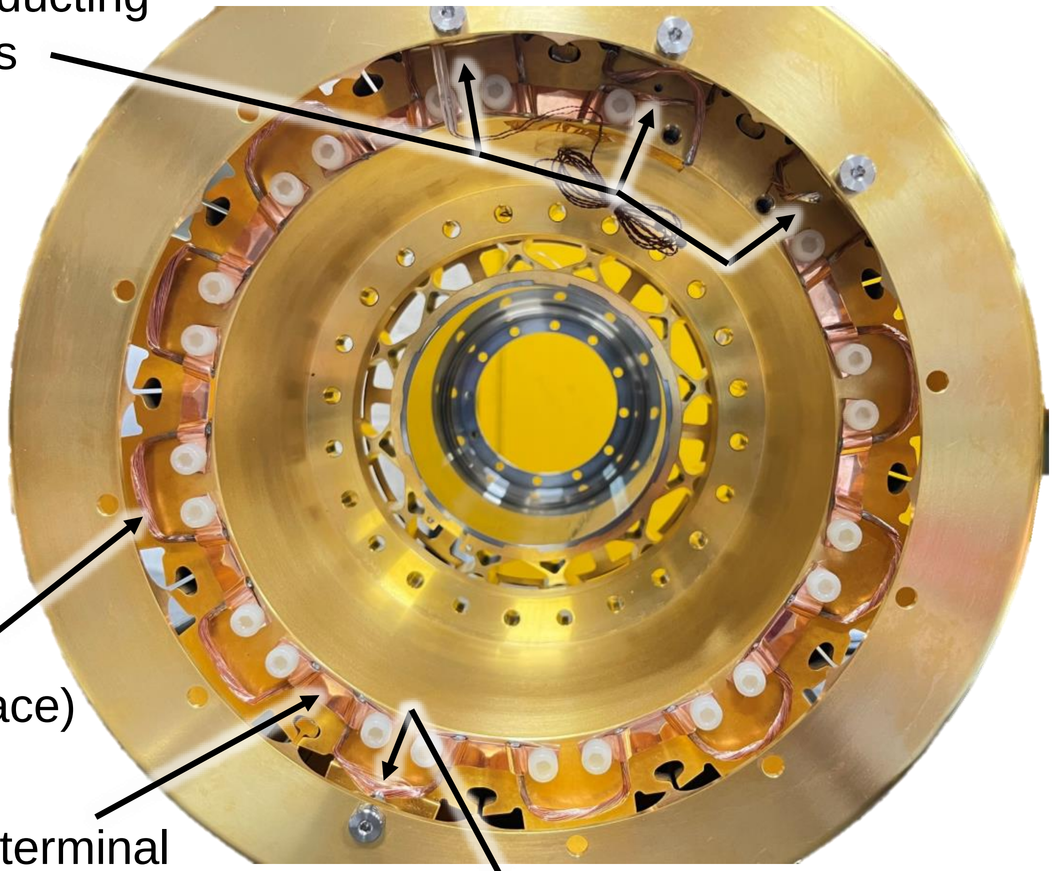

Experimental Setup – Instrumentation

- Vacuum feedthrough channels
  - 15 resistive temperature detectors (RTDs)
  - 9 Type E thermocouples
  - 4 voltage probes
  - 2 heaters
  - 1 pair high current leads

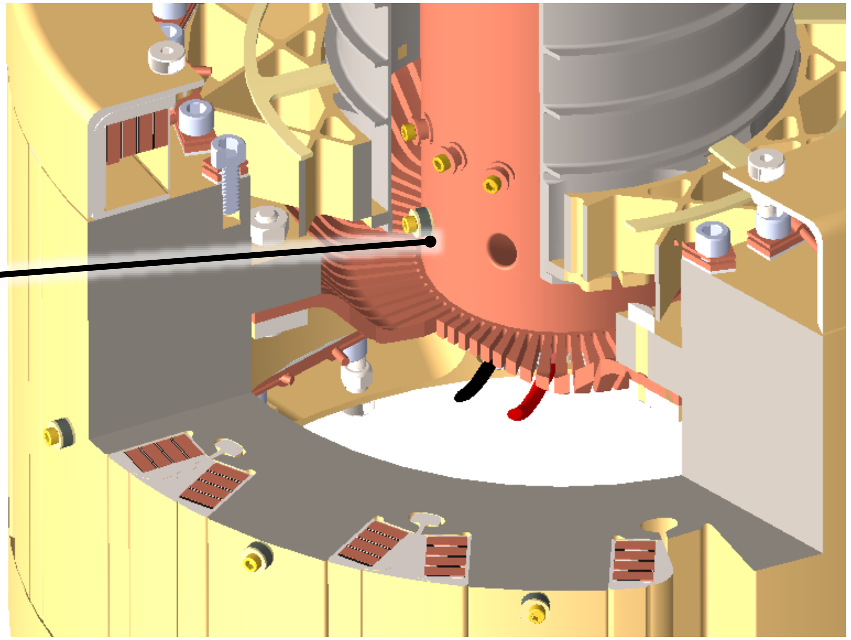

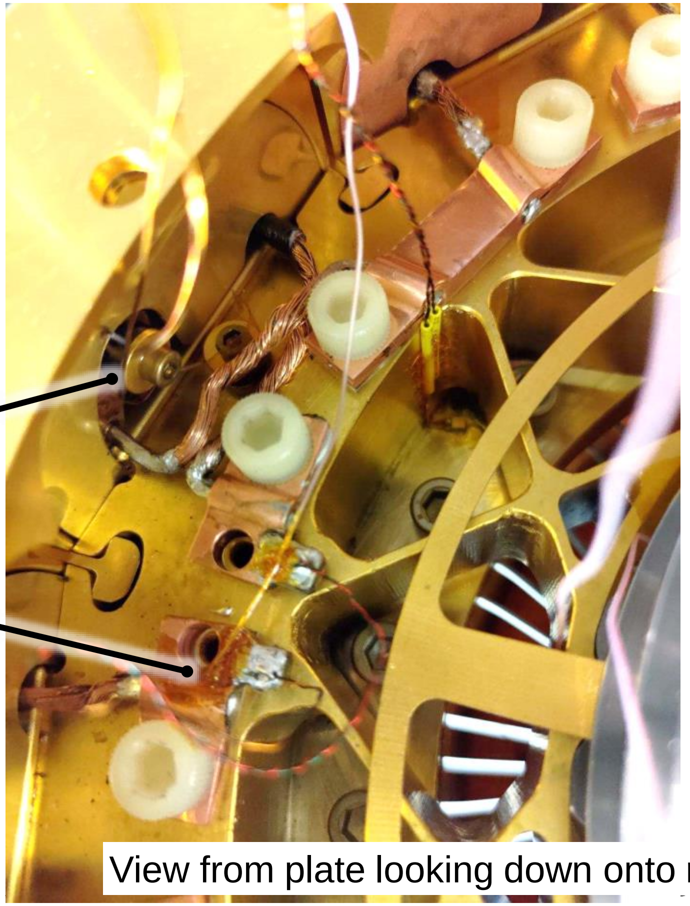

View from plate looking down onto rotor

Experimental Setup – Instrumentation

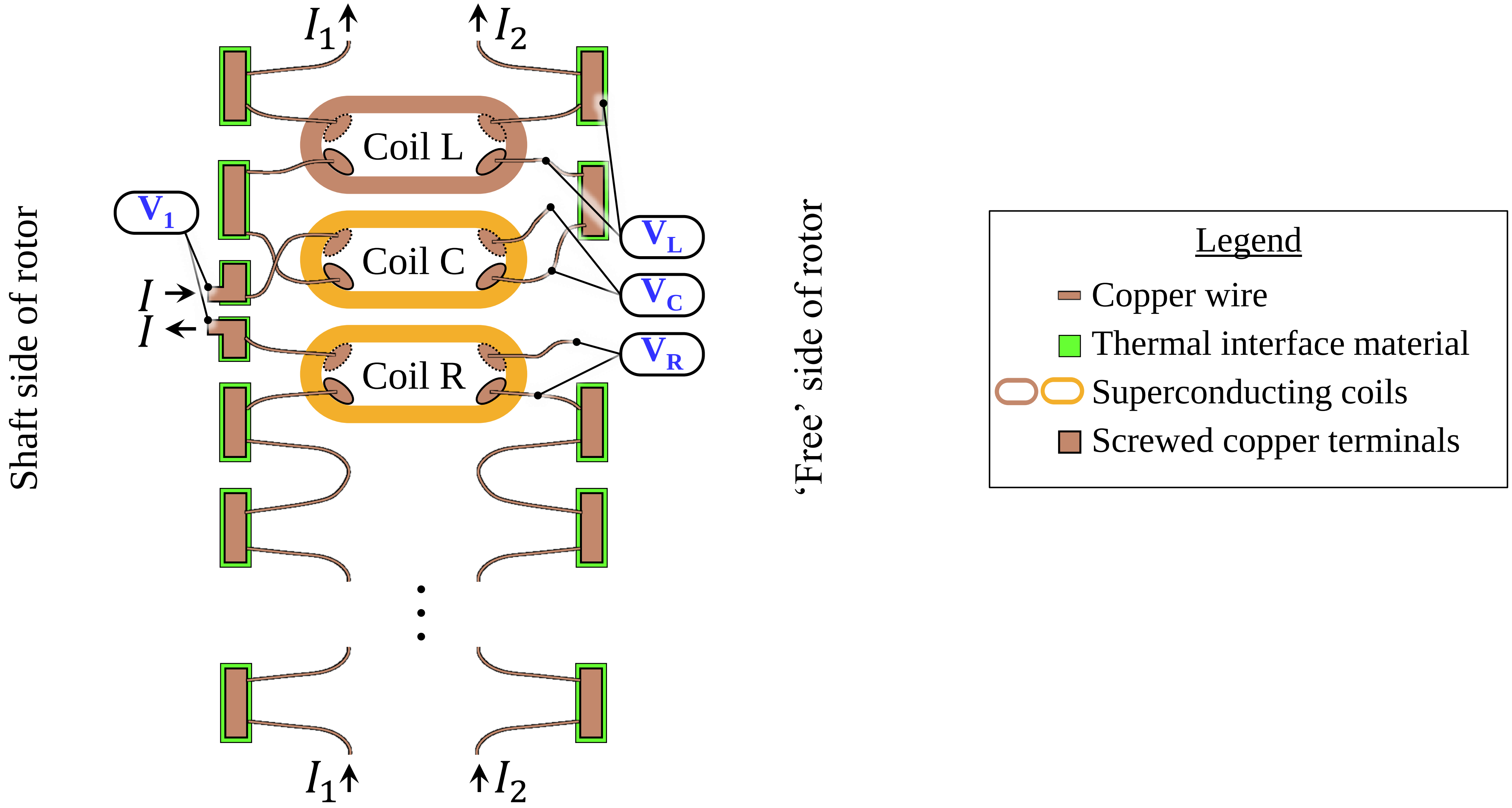

Experimental Results – Electrical

- Current slowly ramped between set points (~ 0.5 – 0.7 A/min) to minimize heating in coils
- Each data point taken after voltage and temperature exhibited little variation (typically 30-45 minutes)
- **1st round of testing**
  1. At 60.5 – 61.0 K
     1. Linear & stable voltage response up to 45 A, then ~7 mV jump while stabilizing at 50 A
     2. Linear & stable voltage up to 57.2 A (rated current)
  2. At 57.2 A
     1. Linear & stable voltage from 60.8 K to 62.0 K (rated temperature)

Electrical Results – Voltage Response

- 2nd round of testing
  - At 60.9 – 61.1 K
    - Linear & stable voltage up to ≥ 47.5 A on 4 separate occasions over 2 weeks

Electrical response of the entire rotor (left) & each superconducting coil (center, right)

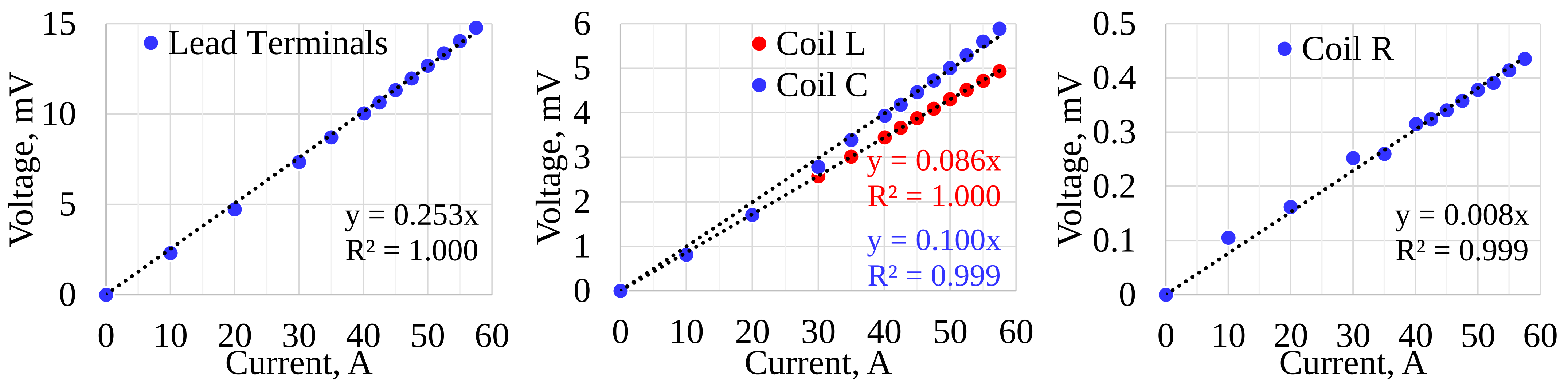

	Entire rotor	Coil L	Coil C	Coil R
Measured Resistance *R*, mOhm	0.253	0.086	0.100	0.008

Electrical Results – Inductance

- 2nd round of testing
  - At 60.9 – 61.1 K
    - Measured exponential time constant (τ): average: 10.2 min | standard deviation: 1.2 min
    - **Estimated inductance = 0.15 H** (series L-R circuit: $L=\tau R$)

Exponential decay of voltage after reaching 9 current set points

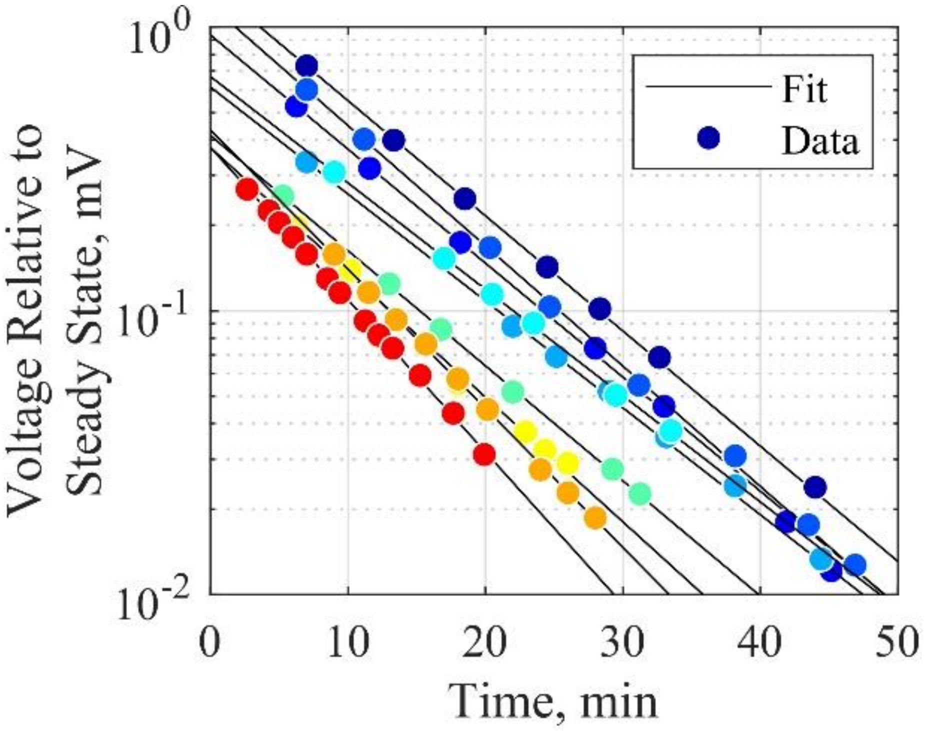

Calculated inductance for solenoid approximation**

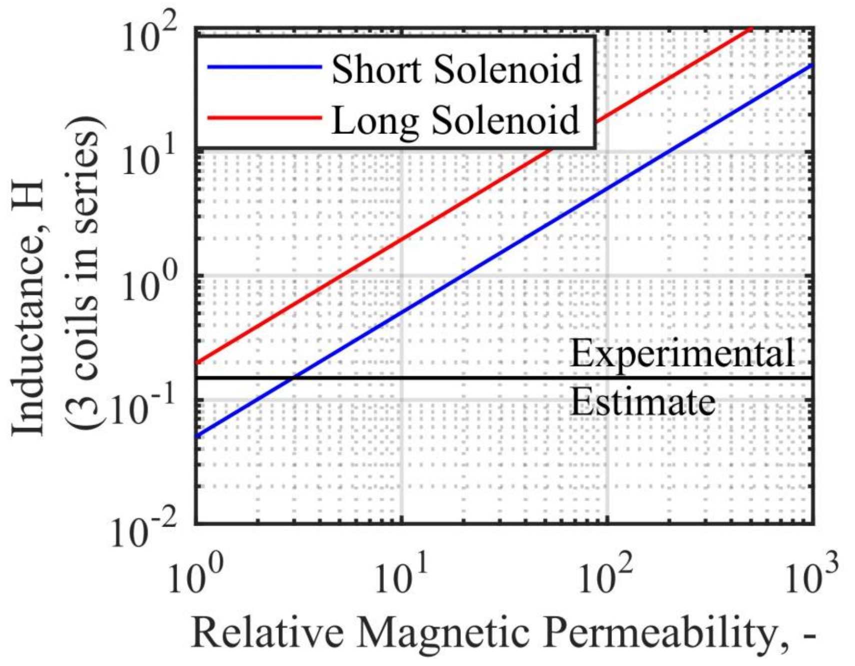

** Long solenoid: $L = \frac{\mu N^2 A}{l}$ Short solenoid: $L = \frac{\mu N^2 A\{\sqrt{a^2 - l^2} - a\}}{l^2}$

N = # of turns = 600 | A = cross-sectional area = $\frac{\pi}{4}(50.8)^2$ mm² (mean diameter of end turns = 50.8 mm) | a = radius of turn = $\frac{50.8}{2}$ mm | l = length = 14 mm

Electrical Results – Inductance

- 2nd round of testing

Voltage response to quasi-step 10 A decrease in current

Coil temperatures, K	Measured time constant, s	Measured resistance, mOhm	Estimated inductance, mH
55.8 to 57.4	628	0.253	159
104.3 to 105.6	< 0.2	0.680	< 0.1
300	< 0.2	0.557	< 0.1

HEMM – Thermal Design

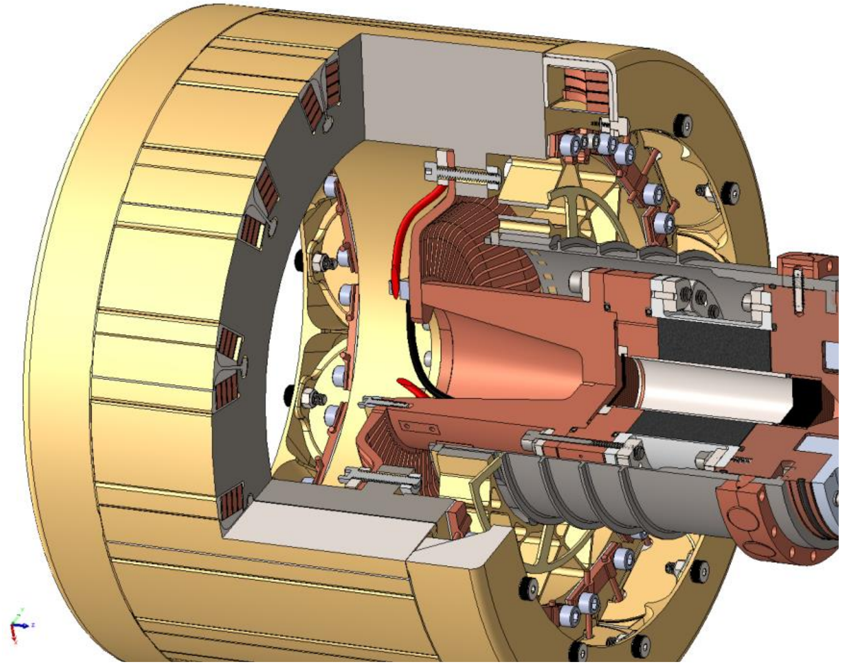

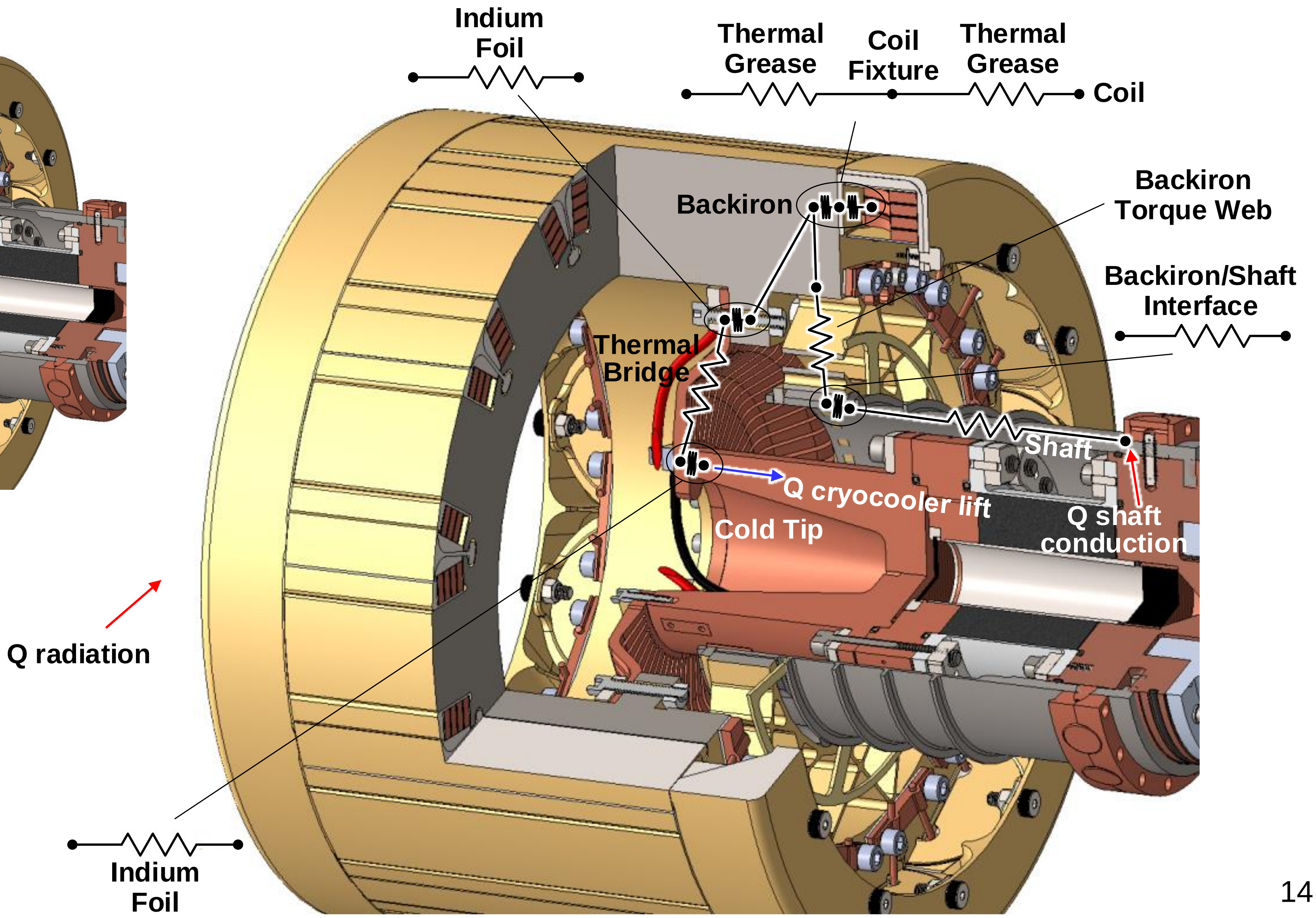

Steady-State Thermal Results

- Steady state: >90% of temperature sensors changing at rate < 0.2 K/hr
- Most tests: cold tip held at 45 K rather than 50 K (HEMM's nominal)
- **Allowable ΔT from cold tip to coils: 12 K**

Test Point	Rotor Current (A)	Support Plate Heater Enabled?	HEMM's Cold Tip Temp. (K)	Coil Temp. (K)		ΔT, Cold Tip to Coils (K)	
				Average	Peak	Average	Peak
A	0	Yes	48.2	59.6	60.2	11.3	12.0
B	0	No	26.3	39.1	40.1	12.9	13.8
C	0	No	45.0	55.9	56.6	10.9	11.6
D	0	No	45.0	55.2	55.9	10.2	10.9
E	47.5	No	45.0	55.8	56.7	10.8	11.7
F	0	Yes	45.0	56.6	57.3	11.6	12.3

After improvements
(to cleanliness, clamping force, instrumentation)

Measured peak ΔT from cold tip to coils (10.9 to 12.3 K) is acceptable, but with no margin

Steady-State Temperature Gradients Across Interfaces

- Values shown for test points C – F (after improvements)
- In most cases, ΔT varied by < 0.6 K between test points
- **Relative to uncorrelated model:**
  - Current terminals hotter
  - Other interfaces similar

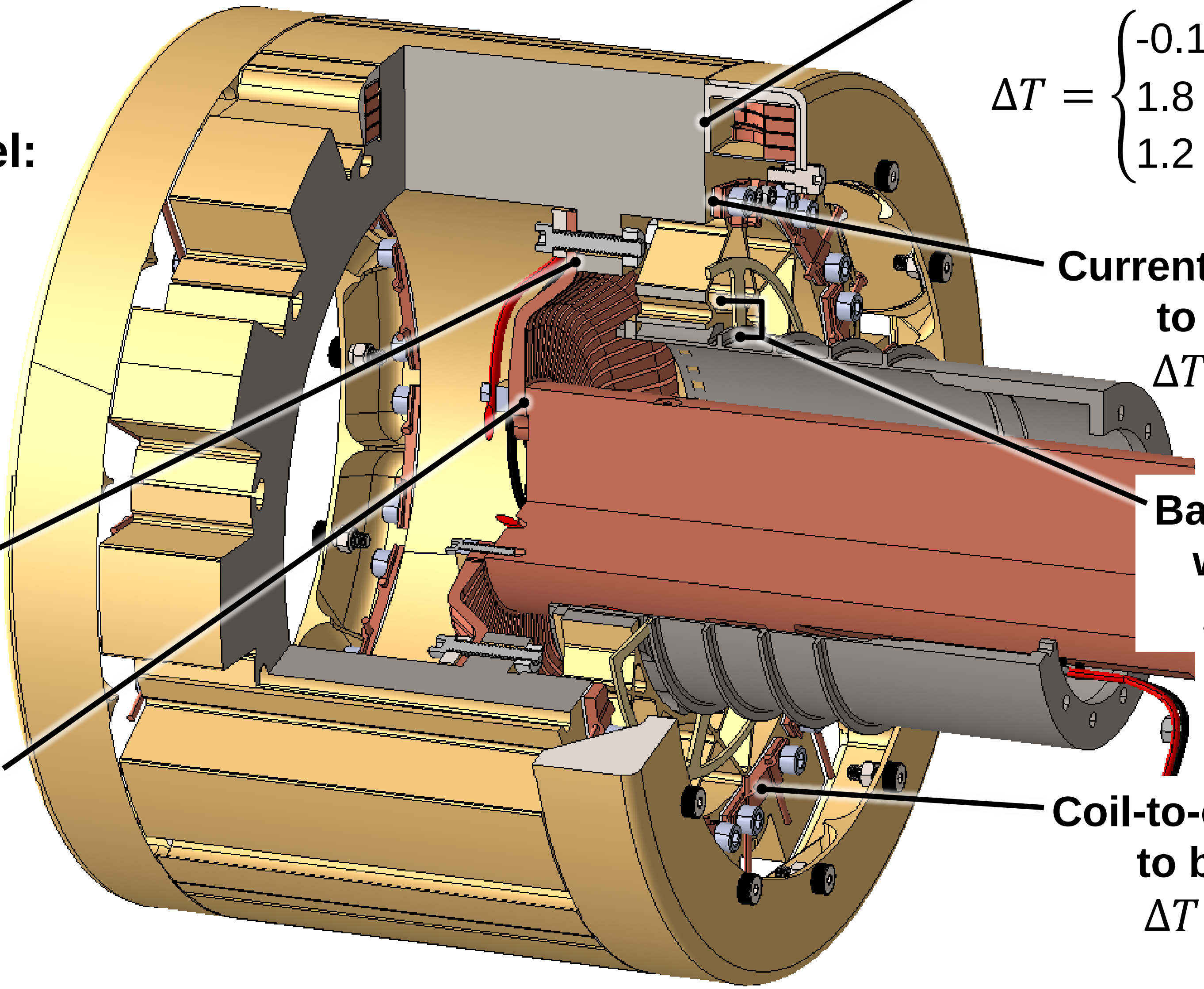

Steady-State Temperature Differences Between Parts

- Values shown for test points C – F (after improvements)
- **Relative to uncorrelated model:**
  - Shaft ΔT considerably lower
  - Dovetail part thermally coupled
  - Hoop less coupled

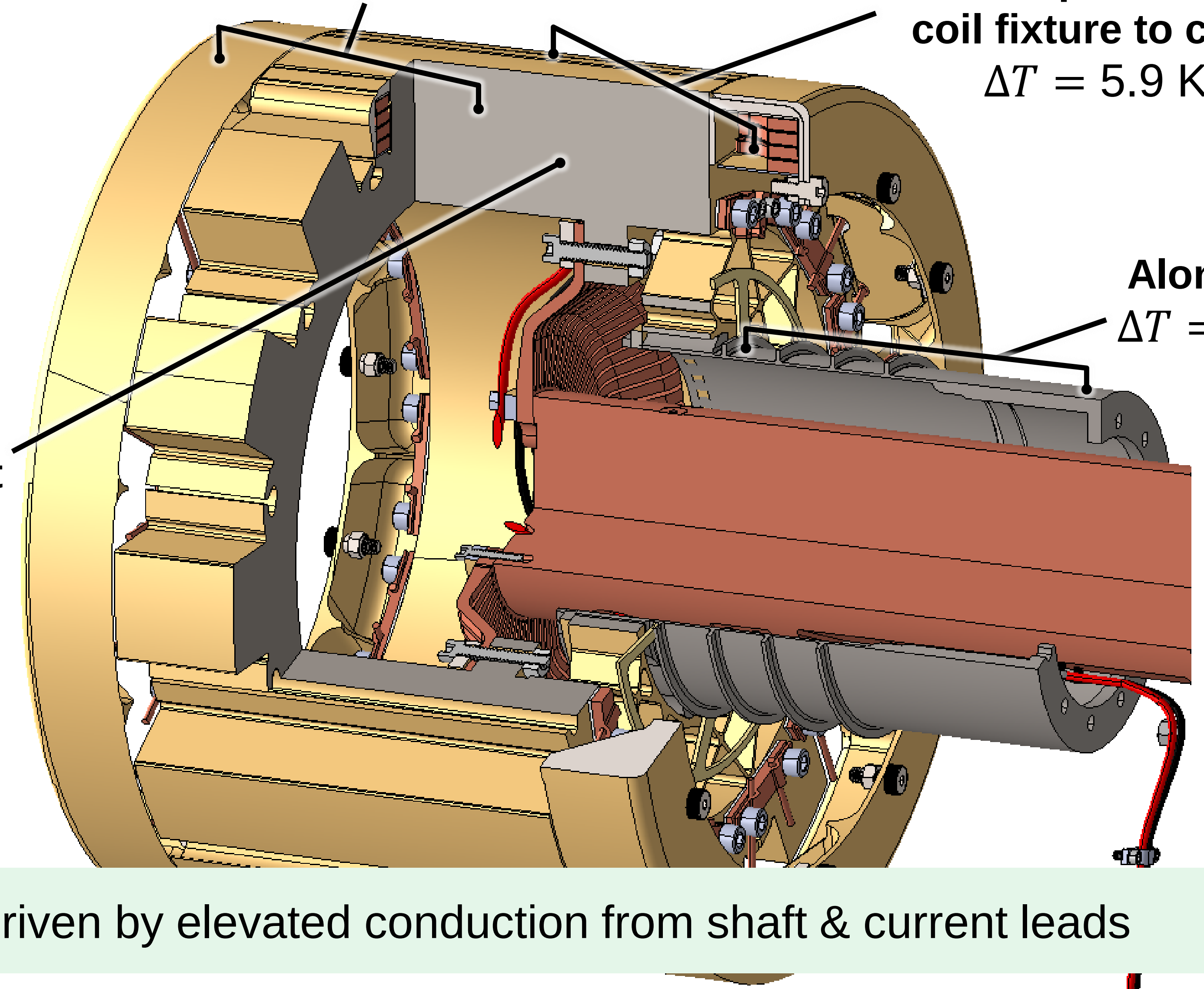

ΔT from cold tip to coils driven by elevated conduction from shaft & current leads

Conclusions

- Thermal & electromagnetic differences between HEMM & ICE-Box experiment are acceptably small [1]
- **Sustained 6 thermal cycles from 293 K to < 50 K throughout test campaign**
- Despite lack of magnetic sensors, **good confidence that superconducting coils operated as intended**
  - Linear & stable operation up to ≥ 45 A in 6 separate tests
  - Estimated inductance of rotor (0.15 H) had reasonable magnitude & went to ~0 above HTS transition temperature
- **ΔT from HEMM's cold tip to coils acceptable but with no margin**
  - Identified opportunities to reduce ΔT

Stable operation of rotor at rated current (57.2 A) and rated temperature (62.0 K) demonstrated while conductively cooled with acceptable ΔT

1st ever demonstration of superconducting rotor cooled conductively without a cryogen

1. Scheidler, J.J. et al., In 2023 IEEE/AIAA Electric Aircraft Technologies Symposium (EATS), San Diego, CA, 2023. https://doi.org/10.2514/6.2023-4537

Acknowledgements

This work was funded by

- NASA's Advanced Air Transport Technology (AATT) Project
  - Electrified Aircraft Powertrain Technologies Subproject

Contact Info

Justin Scheidler	justin.j.scheidler@nasa.gov
Erik Stalcup	erik.j.stalcup@nasa.gov
Thomas Tallerico	thomas.tallerico@nasa.gov
William Torres	william.torres@nasa.gov
Kirsten Duffy	kirsten.p.duffy@nasa.gov

THANK YOU


Glenn Research Center
Lewis Field
RESEARCH AND TECHNOLOGY
NASA
Glenn
Research
Center
FOR THE BENEFIT OF ALL
NASA

Simulated Thermal Response

- Radiation, conductive, and resistive heating loads are applied to ICE-Box model
- 4 W lower heat load in experiment due to lack of windage
  - Thus, generally lower temperatures in experiment
- End winding hoops operate at up to ~100 K due to missing coils

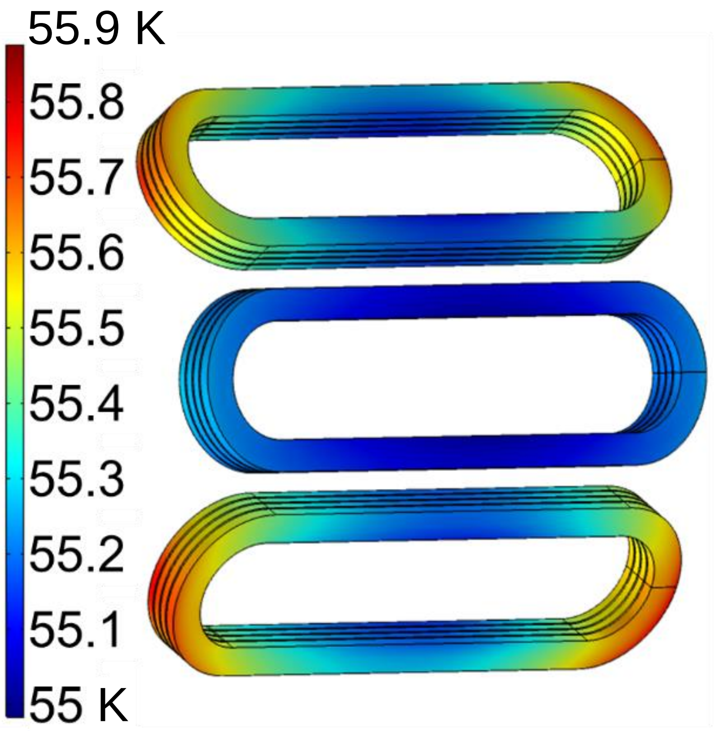

Predicted coil temperatures

	ICE-Box Test	HEMM
Maximum	55.9 K	57.4 K
Average	55.3 K	57.2 K

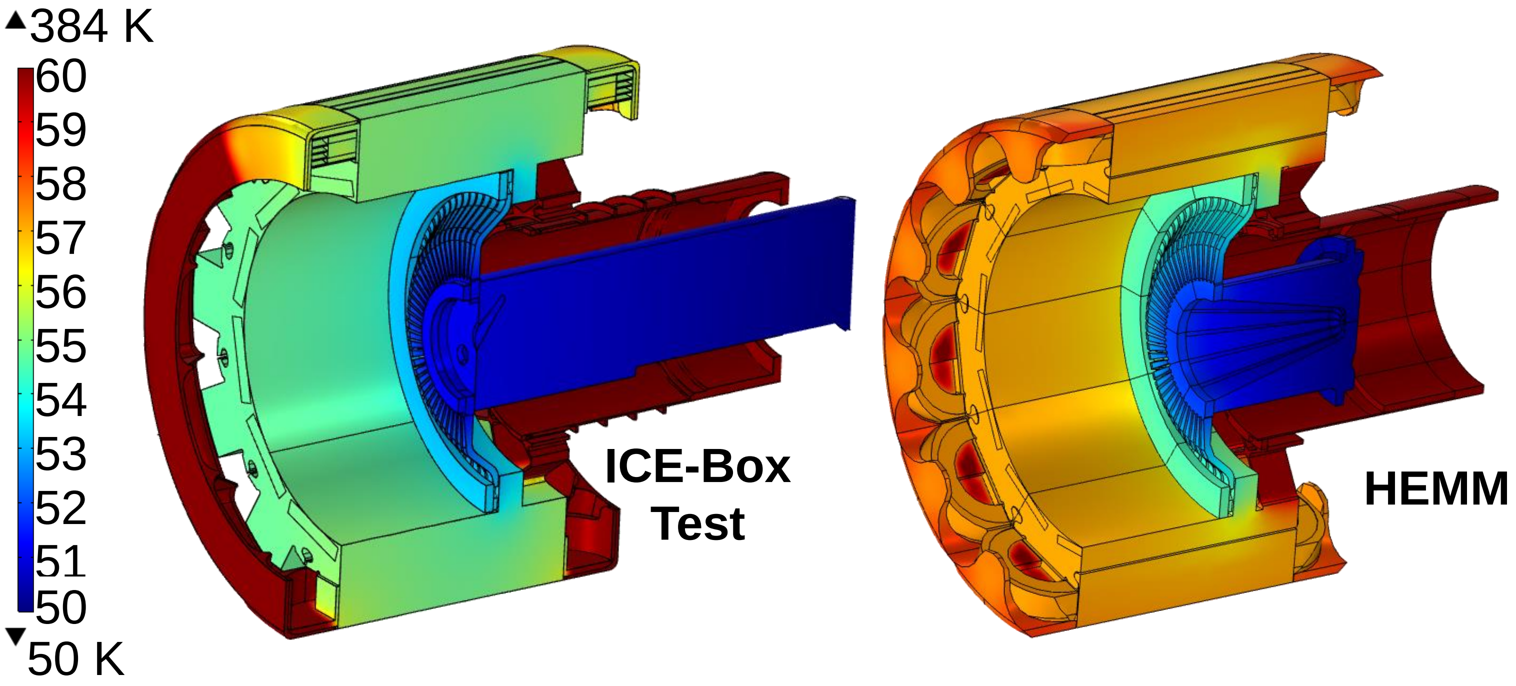

Simulated Electromagnetic Response

- Rotor current & # turns same in both models
- Nonlinearity considered
- Using HEMM design method, critical current in ICE-Box test 2.1 A less than in HEMM

HEMM ICE-Box Test

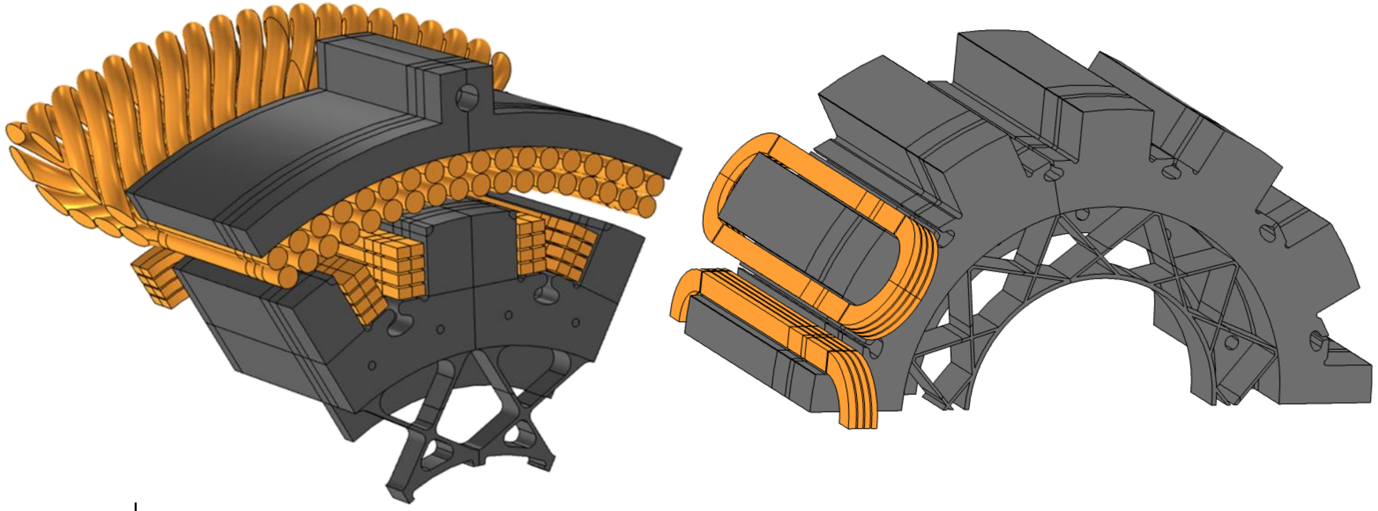

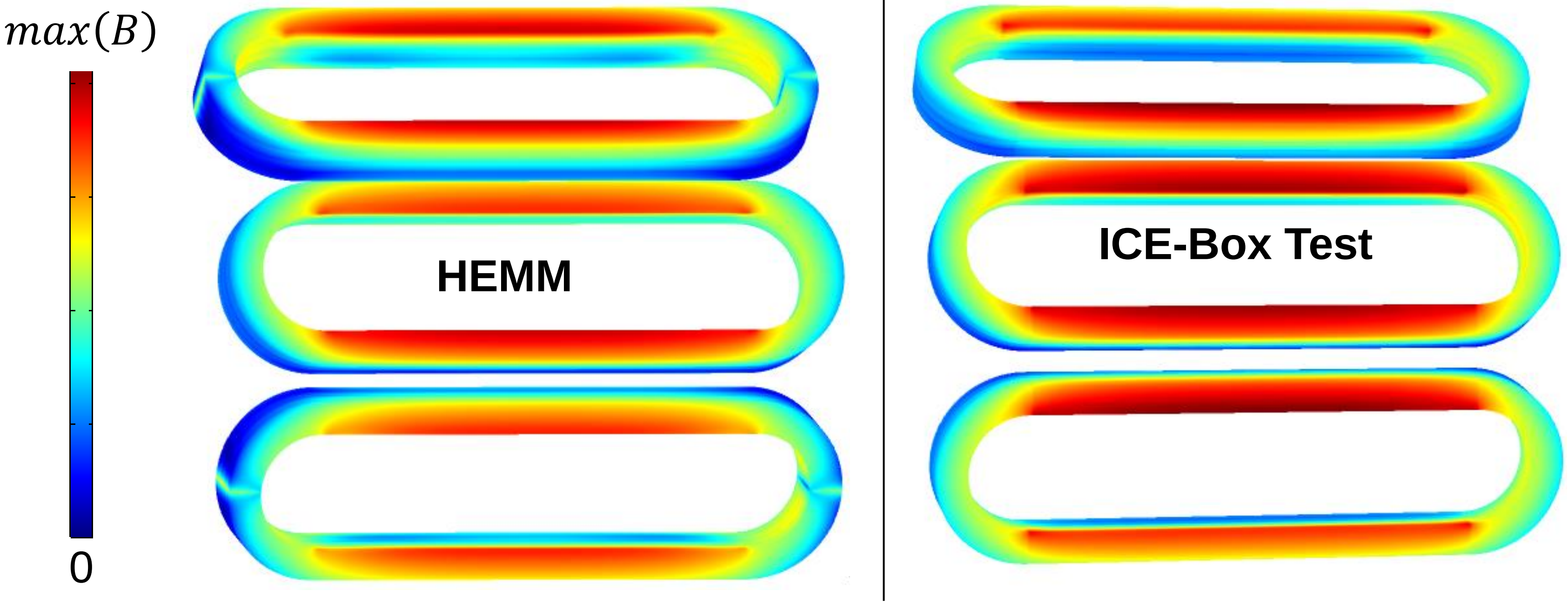

Simulated Electromagnetic Response

- Critical current calculation considers:
  - Temperature from previous slide
  - $I_c(77\ K, s.f.)$ of conductor used to make each layer
- Stator back iron not added to experiment

Predicted critical current (I_c) distribution (units: A) with & without stator back iron

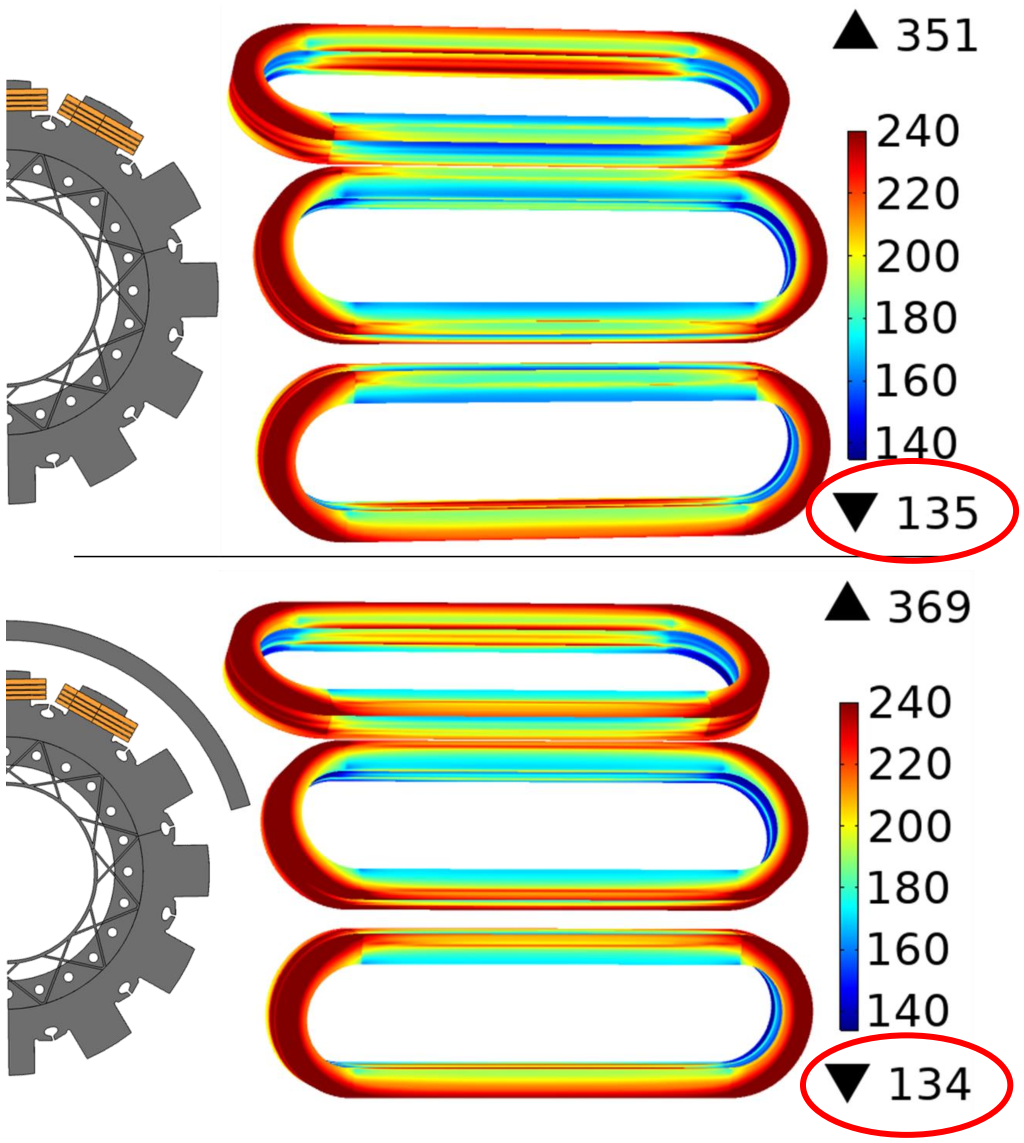

Instrumentation

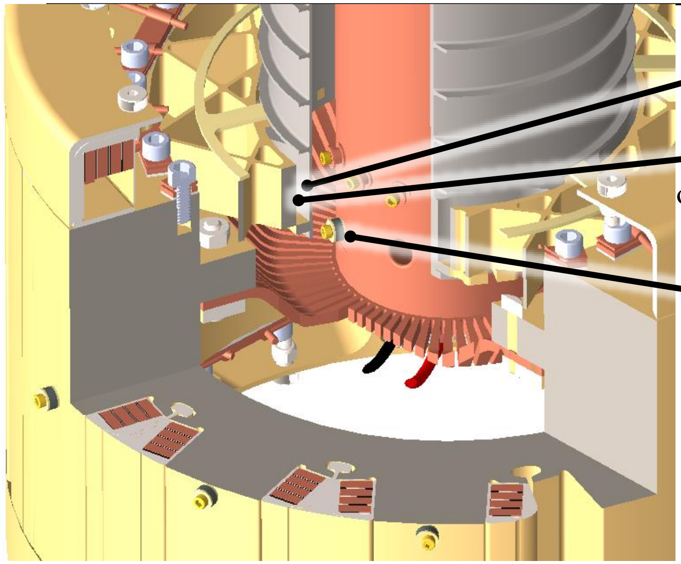

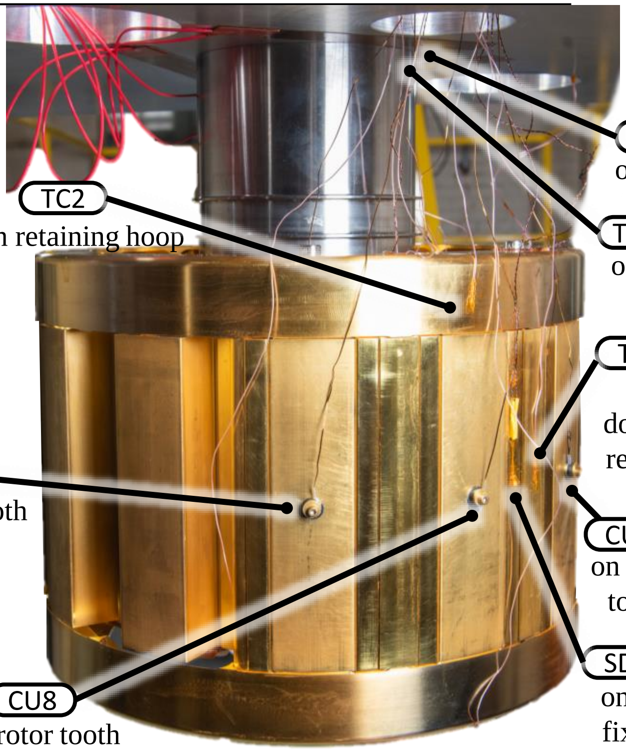

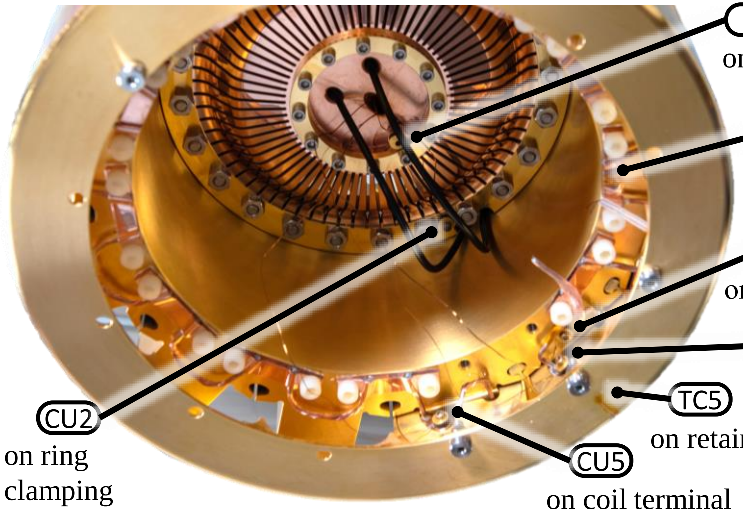

Experimental Results – Electrical

- Current very slowly ramped between set points (about 0.5-0.7 A/min) to minimize heating in coils
- Each data point taken after voltage and temperature exhibited little variation (typically 30-45 minutes)
- Highest temperature in coils controlled to 60.5 to 61.0 K
- ~7 mV voltage jump occurred during 1st attempt at constant 50 A as temperature increased to 61.2 K
- 2nd characterization shows higher resistance but stable at the design current while conductively cooled

Electrical characterization of the entire rotor before (left) & after (right) voltage jump

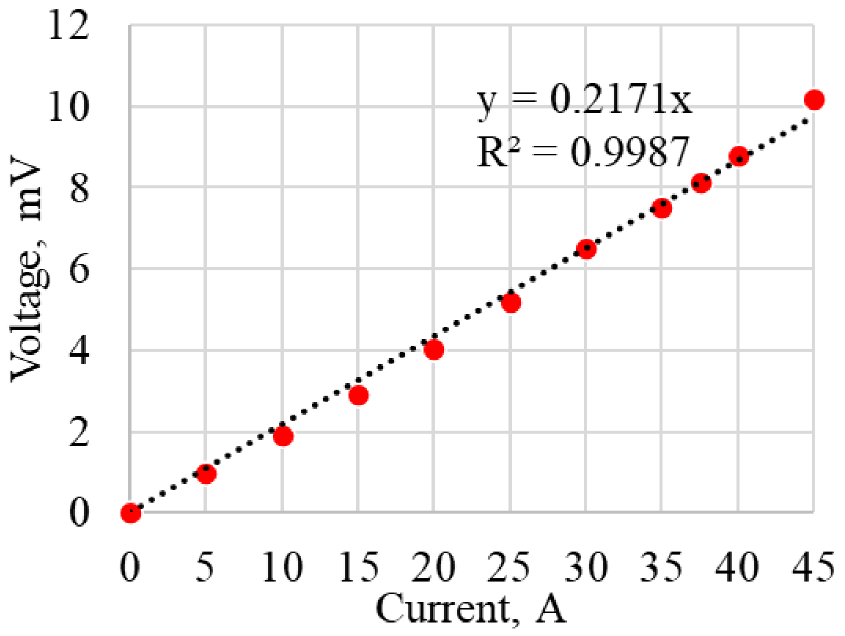

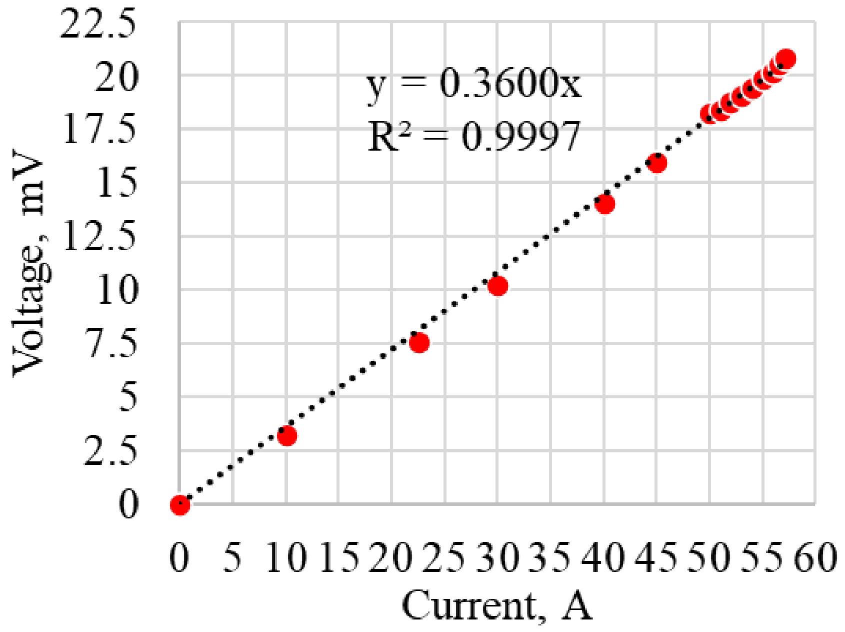

Experimental Results – Electrical

- After stably operating at 57.2 A and 60.9 K, current held fixed, and temperature slowly raised in increments to 62.0 K
- Linear response & increase in voltage (1.40%) suggest superconductivity maintained to 62.0 K (HEMM design limit)

Voltage across the superconducting rotor during a temperature excursion at 57.2 A

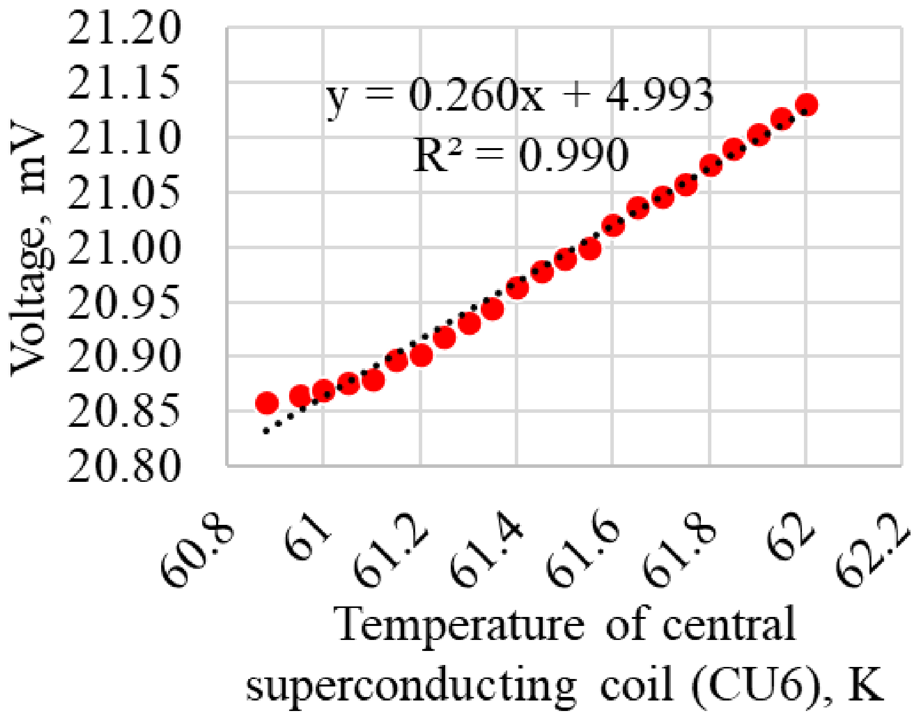

Predicted increase in resistance (thus voltage) per linear interpolation of cryogenic data

Material	Change in resistance (& voltage)
Cu (very high purity)	5.53%
OFHC copper (annealed)	3.88%
OFHC copper (60% cold work)	3.54%
Less pure Cu wire	< 3.5%

Steady-State Thermal Results – Test Point E

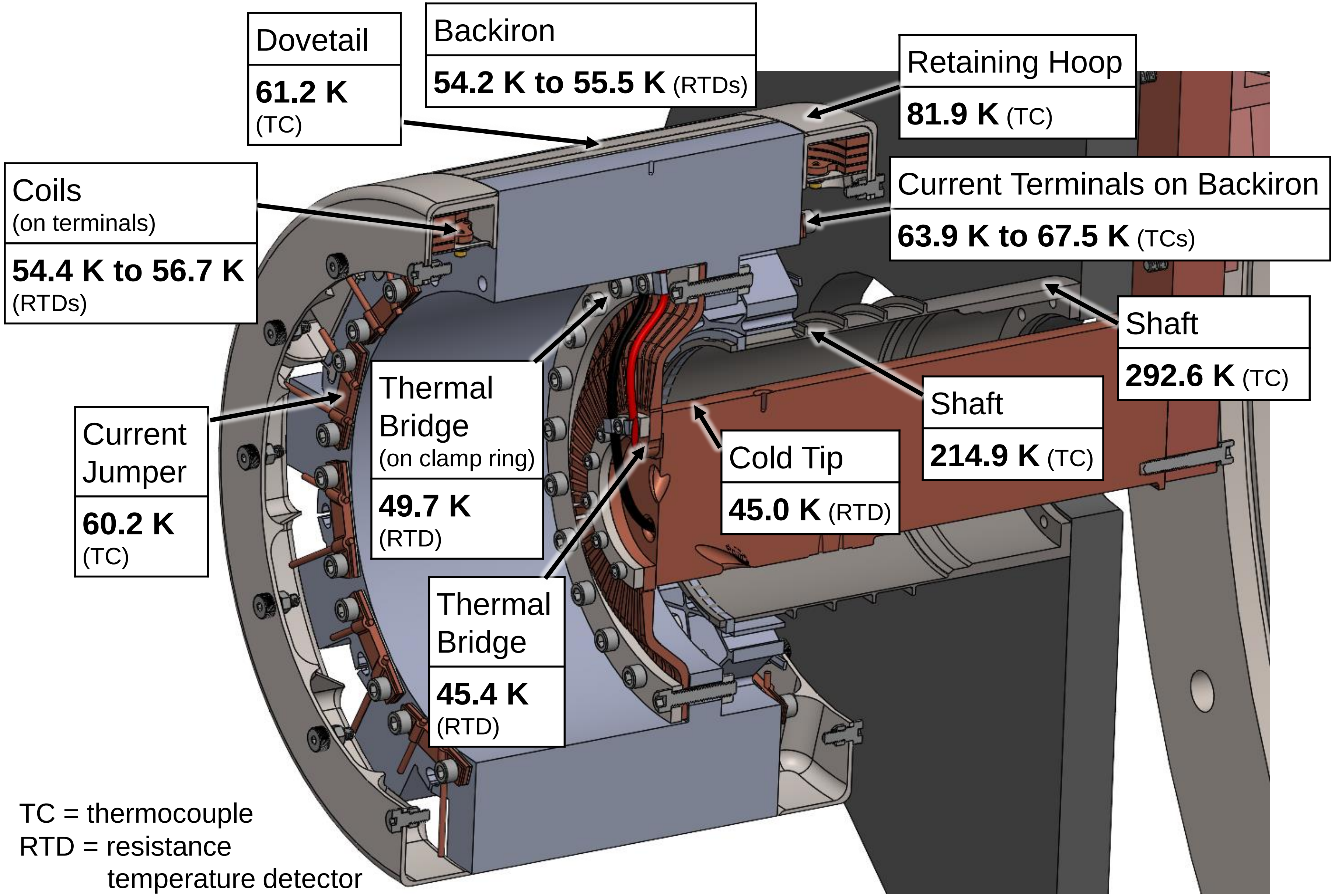

TC = thermocouple
RTD = resistance temperature detector

Steady-State Thermal Results

Notable temperature differences at each test point (location 1 minus location 2)

Location 1	Location 2	Test Point A	Test Point B	Test Point C	Test Point D	Test Point E	Test Point F	Uncorrelated model (test point E)
Cold tip at cold tip/bridge interface	ICE-Box cryocooler cold tip (facility)	12.77	8.77	10.79	10.12	11.01	11.72	–
Thermal bridge at cold tip/bridge interface	Cold tip at cold tip/bridge interface	0.43	0.36	0.41	0.38	0.41	0.45	0.06
Thermal bridge (clamp ring) at bridge/backiron interface	Thermal bridge at cold tip/bridge interface	4.54	4.44	4.28	3.93	4.29	4.53	1.36
Large support plate, near heater	Shaft near interface with Al support plate	65.58	-15.85	-14.79	-17.02	-16.04	59.53	6.54
Shaft near interface with Al support plate	Shaft at shaft/backiron interface	173.18	151.18	86.28	78.79	77.71	60.62	202 (A-B config.) 167 (C-F config.)
Shaft at shaft/backiron interface	Backiron at shaft/backiron interface	26.09	22.04	33.66	4.22	2.44	4.47	3.96
Backiron at shaft/backiron interface	Backiron axial face, coil C, shaft end	37.60	86.47	118.63	155.97	158.22	176.16	16.80
Current lead, terminal A	Backiron axial face, coil C, shaft end	33.63	45.54	8.56	8.80	9.61	13.33	0.23
Current lead, terminal B	Backiron axial face, coil C, shaft end	–	–	10.53	12.42	13.31	15.12	0.27
Coil-to-coil terminal, coil L, free end	Backiron axial face, coil C, free end	9.52	22.28	4.53	5.06	4.73	4.84	-0.07
Coil terminal, coil C, free end	Backiron axial face, coil C, free end	1.36	1.11	1.13	1.18	1.22	1.29	0.46
Coil terminal, coil C, free end	Backiron pole OD, coil C	1.78	1.71	1.74	1.74	1.75	1.87	0.62
Coil terminal, coil L, shaft end	Backiron pole OD, coil L	0.32	-0.50	-0.16	-0.15	-0.25	0.39	0.46
Coil terminal, coil R, free end	Backiron pole OD, coil R	1.20	1.17	1.14	1.17	1.08	1.23	0.45
Coil terminal, coil C, free end	Cold tip at cold tip/bridge interface	12.01	13.71	11.60	10.90	11.69	12.30	3.42
Coil terminal, coil L, shaft end	Cold tip at cold tip/bridge interface	10.31	11.12	9.48	8.97	9.39	10.73	3.36
Coil terminal, coil R, free end	Cold tip at cold tip/bridge interface	11.71	13.80	11.62	10.63	11.33	11.90	3.39
Coil terminal, coil C, free end	Thermal bridge (clamp ring) at bridge/backiron interface	7.03	8.91	6.90	6.59	6.99	7.32	2.00
Coil terminal, coil L, shaft end	Thermal bridge (clamp ring) at bridge/backiron interface	5.34	6.32	4.78	4.65	4.69	5.75	1.94
Coil terminal, coil R, free end	Thermal bridge (clamp ring) at bridge/backiron interface	6.73	9.00	6.92	6.32	6.63	6.92	1.97

Predicted Performance of HEMM’s Cryocooler

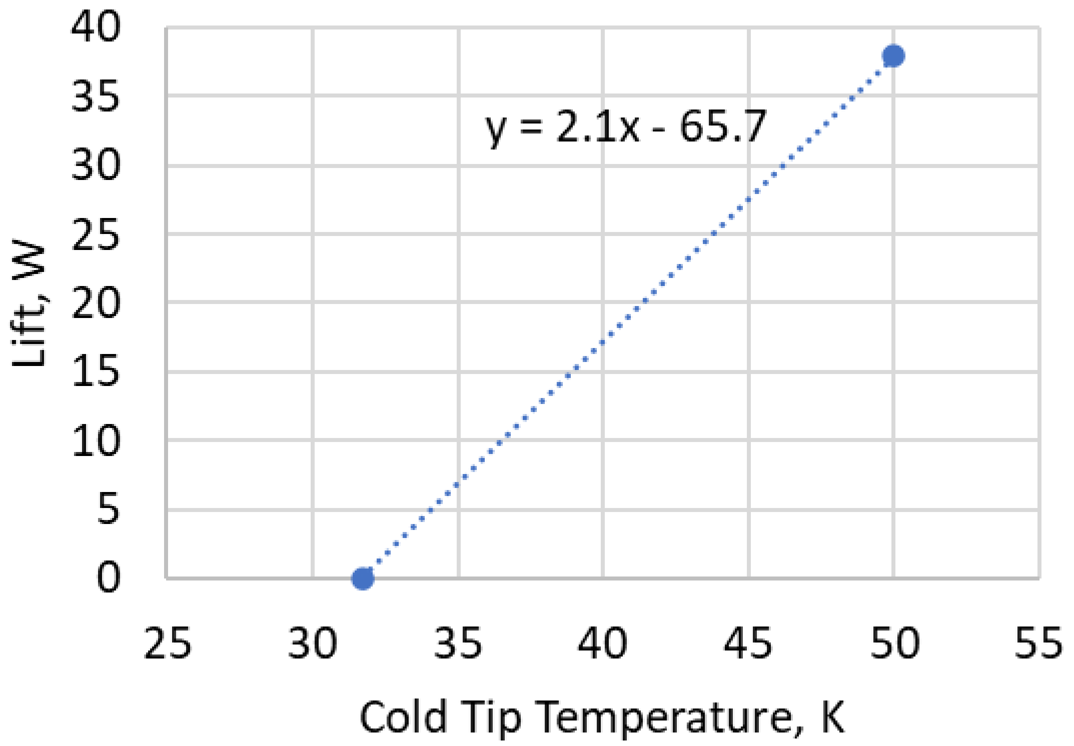

NASA